

Additional file 1

Complete sequencing of *Novosphingobium* sp. PP1Y reveals a biotechnologically meaningful metabolic pattern

Valeria D'Argenio^{1,2,*}, Eugenio Notomista^{3,*}, Mauro Petrillo^{1,2,*},
Piergiuseppe Cantiello¹, Valeria Cafaro³, Viviana Izzo⁴, Barbara Naso^{1,2},
Luca Cozzuto¹, Lorenzo Durante³, Luca Troncone³, Giovanni Paoletta^{1,2},
Francesco Salvatore^{1,5,§}, Alberto Di Donato³

*These authors contributed equally to the work

Corresponding author: Francesco Salvatore

E-mail: salvator@unina.it

¹CEINGE-Biotecnologie Avanzate, Napoli, Italy.

²Dipartimento di Medicina Molecolare e Biotecnologie Mediche, Università di Napoli Federico II; ³Dipartimento di Biologia, Università di Napoli Federico II;

⁴Dipartimento di Medicina e Chirurgia, Università degli Studi di Salerno;

⁵IRCCS-Fondazione SDN, Naples, Italy

TABLE S1 Replication sites in the four PP1Y replicons.

| | <i>OriC/dnaA</i> | <i>parA/parB/parS</i> | <i>repA</i> |
|-----|------------------|-----------------------|-------------|
| Chr | yes/yes | yes/yes/yes | no |
| Mpl | no/no | yes/yes/yes | yes |
| Lpl | no/no | yes/yes/yes | yes |
| Sp1 | no/no | yes/yes/yes* | no |

* Sp1 contains also a *parS/parA/parB/parS* operon (see section entitled “Evaluation of the putative DNA replication origins” in the main text under Results and Discussion)

TABLE S2 Complete list of the PP1Y potential ORFs for the three subunits of the RND-type Efflux Pumps.

| Inner Mem | Membrane-fusion | Outer Mem | periplasm |
|-----------|-----------------|-----------|-----------|
| AT477 | AT501 | | |
| | | AT26323 | |
| AT26892 | AT26745 | AT26928 | |
| | AT26450 | AT26437 | |
| | AT36239 | | |
| | | AT37190 | |
| AT9347 | AT9368 | AT9332 | |
| AT28595 | AT28585 | AT28618 | |
| AT16571 | AT16559 | AT16549 | |
| | AT17967 | AT17956 | |
| Mp12516 | Mp12495 | Mp12540 | |
| | Mp15845 | | |
| | Mp19413 | Mp19442 | |
| AT22882 | AT22868 | AT22851 | AT22908 |
| AT22740 | AT22725 | AT22714 | |
| | AT21473 | AT21444 | |

TABLE S3 PP1Y genes involved in glutathione metabolism.

ORFs AT4214 and AT30465 code for two glutathione peroxidases that could play a role in the detoxification of alkylhydroperoxides. ORFs AT14455 and AT32855 code for lactoylglutathione lyases that catalyze the condensation of glutathione and methylglyoxal to lactoylglutathione. AT13944 codes for hydroxyacylglutathione hydrolase that catalyzes the hydrolysis of glutathione thioesters regenerating free glutathione. AT25438, AT20884 and AT21125 code for enzymes that catalyze the condensation of glutathione and formaldehyde to the corresponding thioacetale (S-hydroxymethyl glutathione). The adjacent ORFs, AT9397 and AT9409, code for a S-hydroxymethyl glutathione dehydrogenase and a S-formylglutathione hydrolase that convert the thioacetale to glutathione and formate. ORF AT9427, close to AT9397 and AT9409, and ORFs AT21359, AT21382 and AT21411 code for the subunits of a formate dehydrogenase that, by oxidizing formate to CO₂, completes the degradation pathway of formaldehyde.

| | |
|---|---|
| AT342 / AT11664 / AT11540 / AT9150 / AT4221 / AT11532 / AT28366 / AT21203 / AT11674 / AT11650 / AT20084 / AT28388 / AT28401 / AT33940 / AT11660 | glutathione S transferase like (15) |
| AT6822 | glutathione transferase zeta 1 / Maleylacetoacetate isomerase |
| AT31634 / AT15656 / AT29345 | glutathione S transferase domain containing |
| AT25438 / AT20884 / AT21125 | glutathione dependent formaldehyde activating (3) $R-S^{\cdot} + H_2CO = R-S-CH_2-OH$ (thioacetal) |
| AT9397 | S hydroxymethyl glutathione dehydrogenase /alcohol dehydrogenase $R-S-CH_2-OH = R-S-CH=O$ (thioester of formic acid) |
| AT9409 | S formylglutathione hydrolase $R-S-CH=O + H_2O = R-S^{\cdot} + HCOOH$ |
| AT4214 / AT30465 | glutathione peroxidase $2R-S^{\cdot} + R'-OOH = R-S-S-R + R'-OH$ |
| AT13944 | hydroxyacylglutathione hydrolase $R-S-CO-R' = R-SH + HOOC-R'$ |
| AT14455 / AT32855 | lactoylglutathione lyase glutathione + methylglyoxal ⇌ hemithioacetal adduct ⇌ (R)-S-lactoylglutathione |
| AT29766 | glutathione reductase |
| AT25503 | glutathione synthetase |

TABLE S4 The four large and five small clusters in PP1Y chromosome A coding for hypothetical glycosyl transferases, synthesis of nucleoside-diphosphate-sugar precursors, polysaccharide polymerases and/or export proteins.

| | |
|---------------|--|
| AT7751 | pssK exopolysaccharide polymerization protein |
| AT7758 | polysaccharide biosynthesis protein |
| AT7767 | glycosyltransferase involved in LPS biosynthesis like protein |
| AT7779 | dolichyl phosphate mannose synthase related protein |
| AT7787 | glycosyl transferase family protein |
| AT7798 | conserved hypothetical protein |
| AT7809 | hexapeptide transferase family protein |
| AT7814 | periplasmic protein involved in polysaccharide export/polysaccharide export outer membrane protein |
| AT7822 | putative glycosyltransferase |
| AT7832 | glycosyltransferase |
| AT7845 | new prediction 34 |
| AT7868 | hypothetical protein/UDPglucose 6 dehydrogenase EC 1.1.1.22 |
| AT7894 | glycosyl transferase family 2 |
| AT7905 | ypch01112 glycosyltransferase |
| AT7911 | glycosyl transferase family 2 |
| AT7930 | ATP binding protein of ABC transporter/ATP binding cassette subfamily B bacterial |
| AT7948 | UDP glucose 4 epimerase |
| AT7958 | NAD dependent epimerase dehydratase family protein/dTDP glucose 4 6 dehydratase EC 4.2.1.46 |
| AT7968 | glycosyl transferase group 1 family protein putative |
| AT7979 | Putative uncharacterized protein |
| AT7986 | FAD dependent oxidoreductase/glycerol 3 phosphate dehydrogenase EC 1.1.5.3 |
| AT7994 | dolichol phosphate mannosyltransferase EC 2.4.1.83 |
| AT8000 | glycosyl transferase family protein |
| AT8011 | glycosyl transferase family protein |
| AT8041 | NAD dependent epimerase dehydratase putative |
| AT8050 | methyltransferase putative |

| | |
|----------------|--|
| AT10096 | glycosyl transferase group 1 |
| AT10111 | putative glycosyltransferase protein |
| AT10122 | putative sugar nucleotide epimerase dehydratase protein |
| AT10133 | putative NDP hexose 3 C methyltransferase protein |
| AT10144 | C methyltransferase |
| AT10159 | lpcA galactosyltransferase protein |
| AT10170 | new prediction 50 |
| AT10175 | pssL exopolysaccharide polymerization and or export protein |
| AT10188 | glycosyl transferase family 2 |
| AT10201 | cellulose biosynthesis protein CelD |
| AT10209 | glycoside hydrolase family 16 |
| AT10230 | protein involved in cellulose biosynthesis CelD like protein |
| AT10241 | beta hydroxylase aspartyl asparaginyl family protein |
| AT10248 | ypch01194 glycosyltransferase |
| AT10257 | new prediction 51 |
| AT10266 | glycosyl transferase group 1 |
| AT10272 | conserved hypothetical protein |
| AT10294 | conserved hypothetical protein |
| AT10309 | rfbP undecaprenyl phosphate galactosephosphotransferase |
| AT10321 | polysaccharide export outer membrane protein |

| | |
|----------------|--|
| AT33104 | mannosyltransferase |
| AT33116 | conserved hypothetical protein |
| AT33128 | polysaccharide biosynthesis protein putative |
| AT33142 | conserved hypothetical protein |
| AT33150 | new prediction 148 |
| AT33153 | exoY succinoglycan exopolysaccharide synthesis protein |
| AT33162 | conserved hypothetical protein |
| AT33178 | polysaccharide pyruvyl transferase |

| | |
|----------------|--|
| AT21571 | polysaccharide export protein Periplasmic protein involved in polysaccharide export |
| AT21576 | lipopolysaccharide biosynthesis Chain length determinant protein ; |
| AT21592 | putative exopolysaccharide biosynthesis protein; |
| AT21603 | conserved hypothetical protein |
| AT21618 | ATPase Type II secretory pathway |
| AT21629 | polysaccharide deacetylase |
| AT21636 | glycosyl transferase group 1 |
| AT21638 | conserved hypothetical protein |
| AT21661 | ABC transporter related |

| | |
|--------------|------------------------------|
| AT942 | glycosyl transferase group 1 |
| AT955 | O antigen polymerase |

| | |
|--------------|---|
| AT749 | Transglycosylase SLT domain protein |
| AT752 | UTP glucose 1 phosphate uridylyltransferase |
| AT764 | UDP N acetylglucosamine 1 carboxyvinyltransferase/ UDP-N-acetylglucosamine enolpyruvyl transferase |

| | |
|--------------|---|
| AT837 | sugar transferase |
| AT851 | OstA like protein/ lipopolysaccharide export system protein LptA |
| AT855 | lipopolysaccharide export system protein LptC |

| | |
|----------------|---|
| AT12196 | glycosyl transferase family 14 |
| AT12206 | polysaccharide biosynthesis protein/ Membrane protein involved in the export of O-antigen and teichoic acid |
| AT12221 | glycosyl transferase family 2 |

| | |
|----------------|---|
| AT20178 | dolichyl phosphate beta D mannosyltransferase |
| AT20190 | glycosyl transferase family protein Dolichyl-phosphate-mannose-protein O-mannosyl transferase |

TABLE S5 Three small clusters of ORFs on megaplasmid B coding for hypothetical glycosyl transferases, synthesis of nucleoside-diphosphate-sugar precursors, polysaccharide polymerases and/or export proteins.

| | |
|----------------|---|
| Mpl1952 | polysaccharide deacetylase |
| Mpl1955 | glucose galactose transporter/ fucose permease; |
| Mpl1975 | glycosyl transferase group 1 |
| Mpl1986 | conserved hypothetical protein |
| Mpl1995 | conserved hypothetical protein |
| Mpl2000 | glycosyl transferase group 1 |

| | |
|----------------|--|
| Mpl9979 | glycosyl transferase group 1 |
| Mpl9992 | inner membrane protein YghQ; Membrane protein involved in the export of O-antigen and teichoic acid |

TABLE S6 Distribution of glycosyl hydrolases and glycosyl transferases among sphingomonadales and related groups of alpha proteobacteria, including strain PP1Y.

| | PP1Y | L-1 | UT26 | RW1 | SYK-6 | DSM 12444 | RB-22 56 |
|----|------|-----|------|-----|-------|--------------|-------------|
| GH | 53 | 32 | 43 | 16 | 21 | 44 | 25 |
| GT | 57 | 55 | 54 | 53 | 50 | 32 | 15 |

| | ATCC 10988 | HTCC 2594 | | | | | |
|----|---------------|--------------|--|--|--|--|--|
| GH | 13 | 19 | | | | | |
| GT | 20 | 22 | | | | | |

GH: glycosyl hydrolases
 GT: glycosyl transferases

STRAINS

L-1: *Sphingobium chlorophenolicum*

UT26: *Sphingobium japonicum*

RW1: *Sphingomonas wittichii*

SYK-6: *Sphingobium sp.*

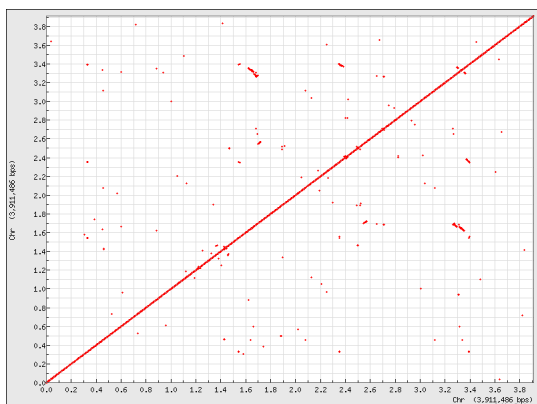
DSM12444: *Novosphingobium aromaticivorans*

RB2256: *Sphingopyxis alaskensis*

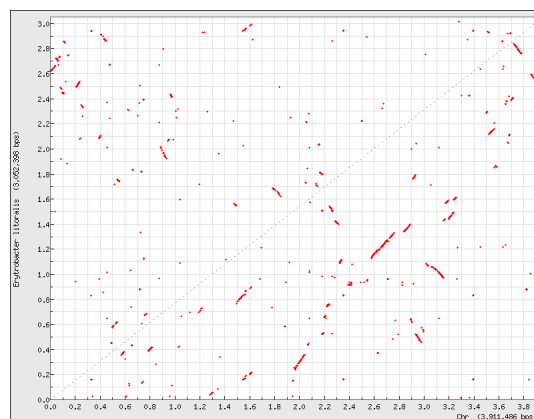
ATCC10988: *Zymomonas mobilis mobilis*

HTCC2594: *Erythrobacter litoralis*

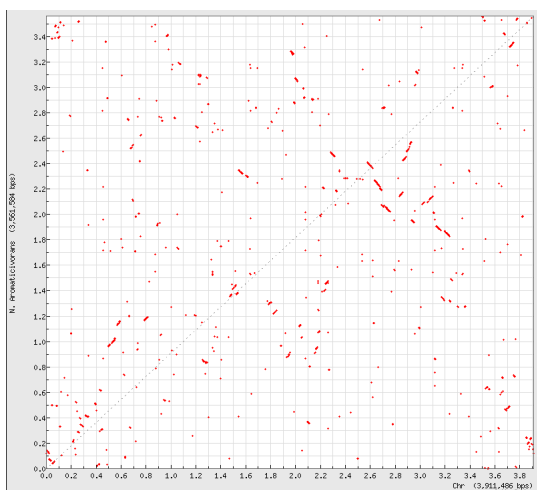
Supplementary Figure S1



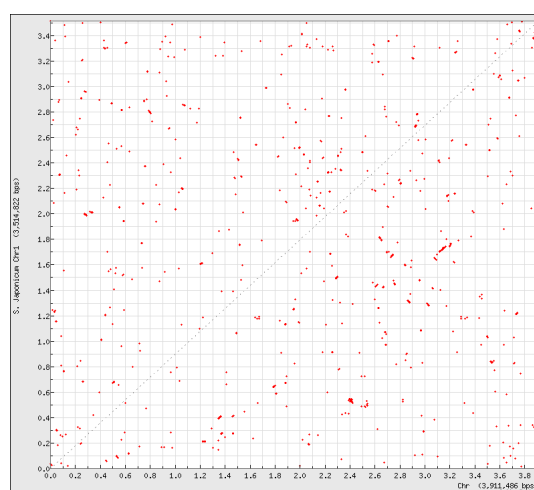
A



B



C



D

FIG S1 Dotplots of PP1Y Chr. The Chr proteome was compared with itself (A), and with those of *Erythrobacter litoralis* (B), *Novosphingobium aromaticivorans* DSM 12444 (C), and *Sphingonium japonicum* (D).

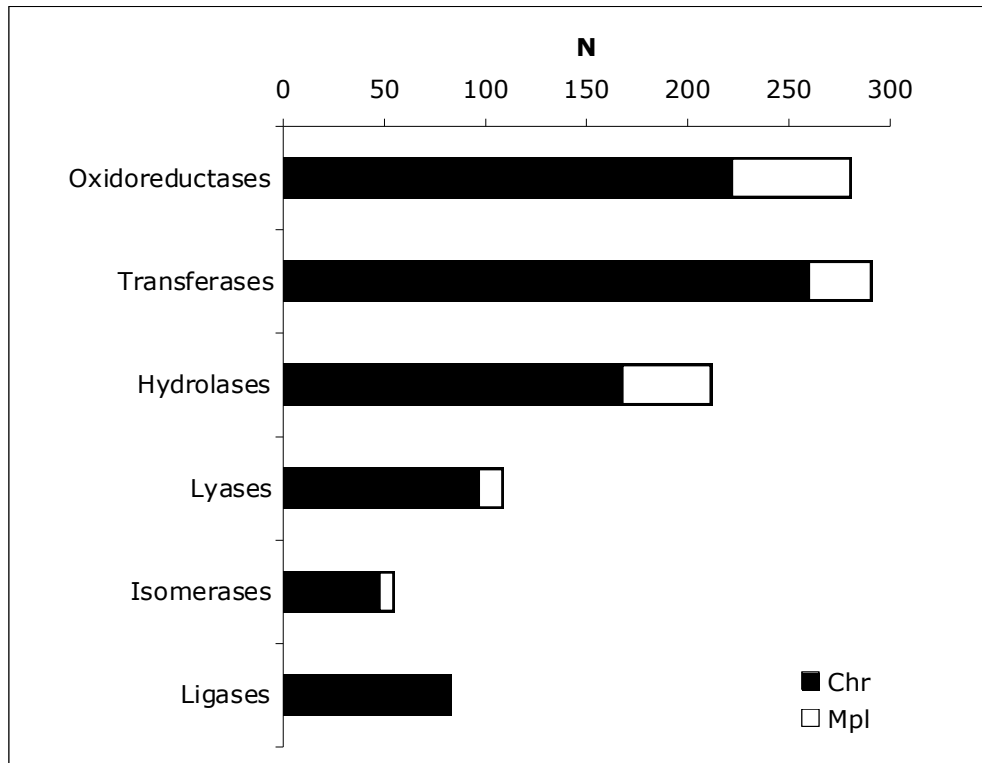
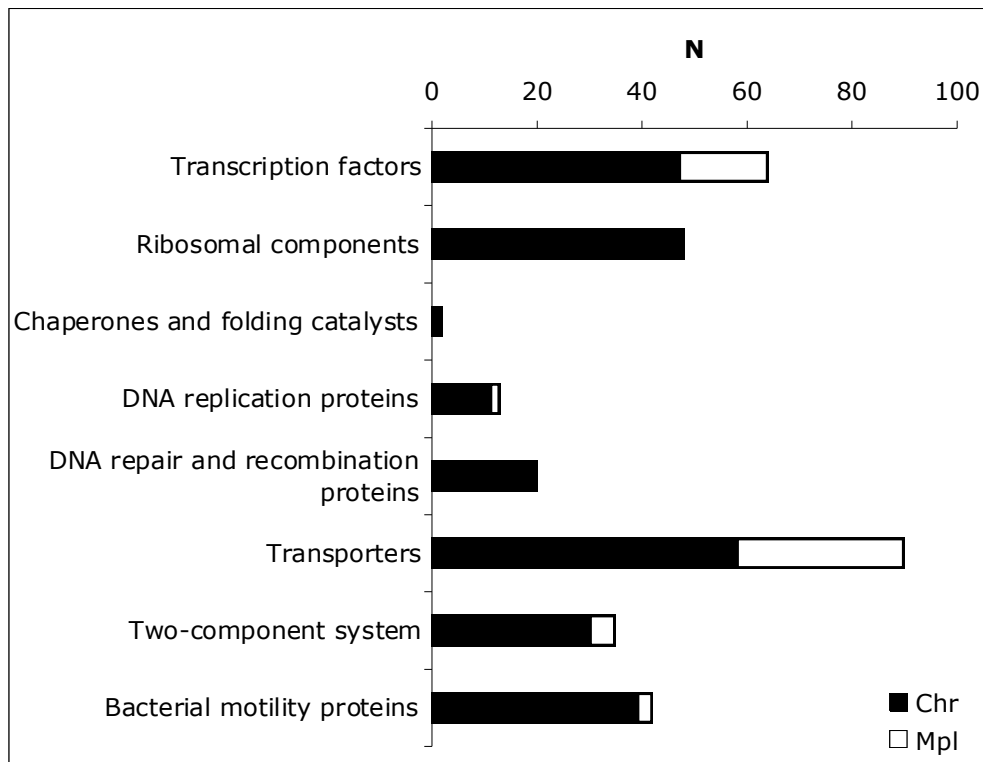
A**B**

FIG S2 Genes and proteins. Distribution of Chr and Mpl genes with respect to enzyme classes (A) and most frequently found protein families according to KAAS (B). N, number of genes.

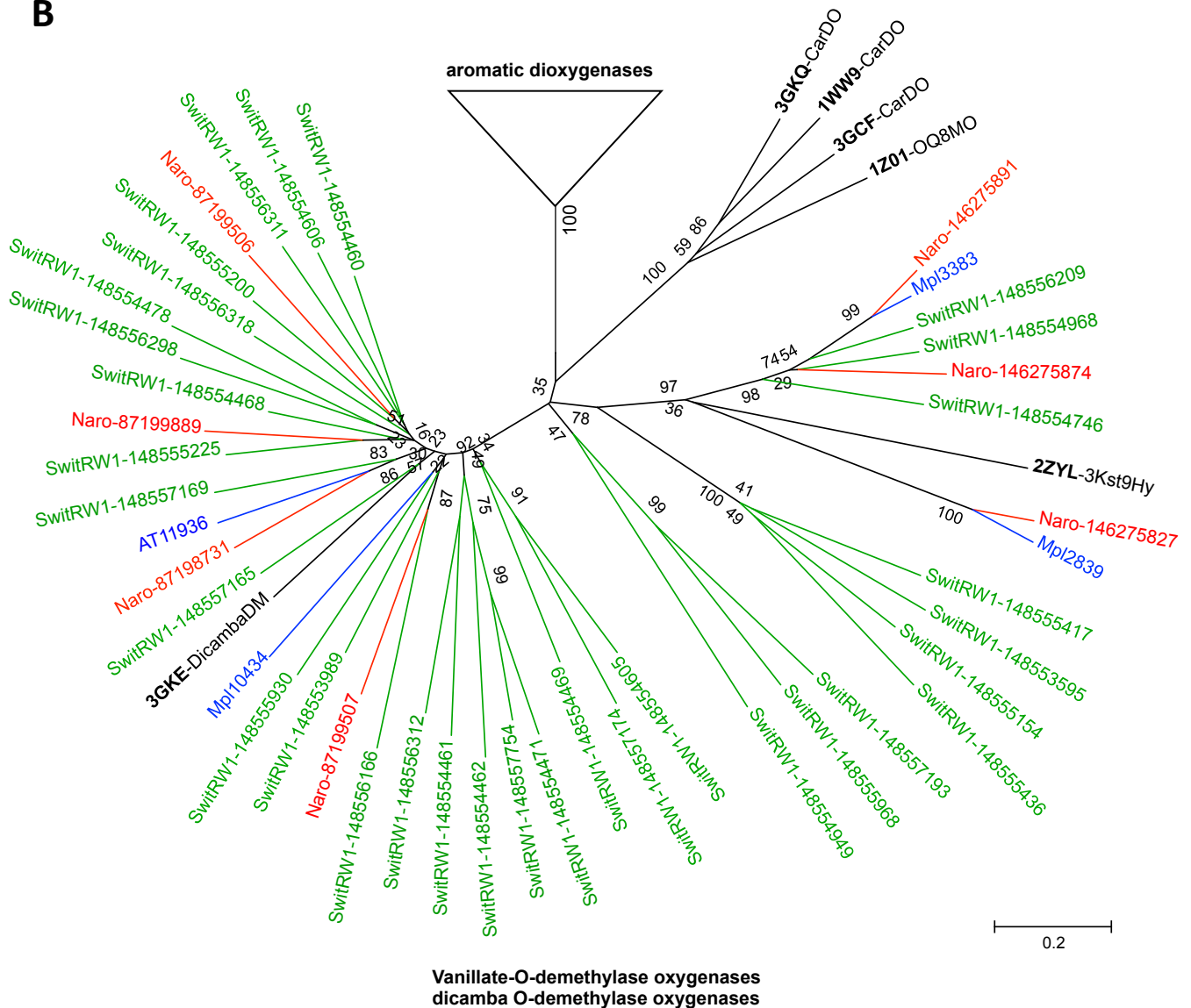
B

FIG S4 Neighbor-Joining tree summarizing the relationships between the alpha subunits of the oxygenases of strains PP1Y (blue), F199 (red), RW1 (green) and L-1 (magenta) and some dioxygenases whose structure has been determined (black). The analysis involved 146 amino acid sequences. For the sake of clarity the two divergent branches of the tree are shown separately in panels A and B. The genome of strain L-1 codes for only 6 oxygenases all in the branch of panel A. The genome of strain RW1 codes for 26 potential dioxygenases (panel A) and 32 potential oxygenases/demethylase (panel B). The numbers in the names of the oxygenases from *shingomonadales* refer to the *gi* accession numbers of the NCBI protein database. PDB codes are in bold. BiphDO, biphenyl-DO; CumDO, cumene-DO; TolDO, toluene-DO; NBenDO, nitrobenzene-DO; NapDO, naphthaleneDO; PAHDO, PAH-DO; QAmDM, quaternary ammonium-demethylase; CarDO, carbazole-DO; OQ8MO, 2-Oxoquinoline 8-Monooxygenase; 3Kst9Hy, 3-ketosteroid-9-alpha-hydroxylase, DicambaDM, Dicamba (3,6-dichloro-2-methoxybenzoic acid) demethylase.

```

PP38178,      1 MDALRYFLVPAMTLTGVAGFILGGPFVWLGIATFAVLMLLDIVLPSDHKARSRGIALVAD
PP37257,      1 MDALRYFLVPAMTLTGVAGFILGGPFVWLGIATFAVLMLLDIVLPSDHKVRSRGIAPVAD
                *****
                *****

PP38178,      61 IAIYLQFPLMVALYLAFANSVATGTNPIWGTDGSAWQLIGSIASLAWLSAVPTLPVAHEL
PP37257,      61 IAIYLQLPLIVALYLAFANSVVSGTNPIWGADGSAWQLIGSIASLAWLSAVPTLPVAHEL
                ***** ** *****
                *****

PP38178,      121 MHRRHWFPRAVAKGLSAFYGDPNRDVAHIVTHHVHLDTAKDSDTPLRQTIYSFVFQATW
PP37257,      121 MHRRHWFPRAVAKGLSAFYGDPNRDVAHIVTHHVHLDTAKDSDTPLRQTIYSFVFQATW
                *****
                *****

PP38178,      181 GSYKDTWEKQGEILSRLGHSPWSWRNAMWLQLVLVGAIILGVAAAAGPIAGFATVGAMFF
PP37257,      181 GSYKDTWEKQGEILTRLGYSPWSWRNAMWLQLVLVGAIILGVAAAAGPIAGFATFGAMFF
                ***** ** *****
                *****

PP38178,      241 AKMFVEGFNYFQHYGLLRVEGDPIAKHHAWNHLGMIVRPIGVEITNHINHHLDGHIPFYE
PP37257,      241 AKMFVEGFNYFQHYGLLRVEGDPIAKHHAWNHLGMIVRPIGVEITNHINHHLDGHIPFYE
                *****
                *****

PP38178,      301 LQPEPKAPQMPSLFLCFLCLGLVPPVWHRFIAQPRLKDWDLHFASPSERKLAMAANAQAGW
PP37257,      301 LQPEPKAPQMPSLFLCFLCLGLVPPVWHKFIAQPRLKDWDLHFASSTERQLAMAANARAGW
                *****
                ***** ** *****

PP38178,      361 PAWATTD
PP37257,      361 PAWATTD
                *****

```

FIG S5 Pairwise alignment between the two potential membrane monooxygenases of strain PP1Y. The differences are shown in red, hypothetical transmembrane helices in green, catalytic residues in blue. The red line indicates the hypothetical substrate binding region.

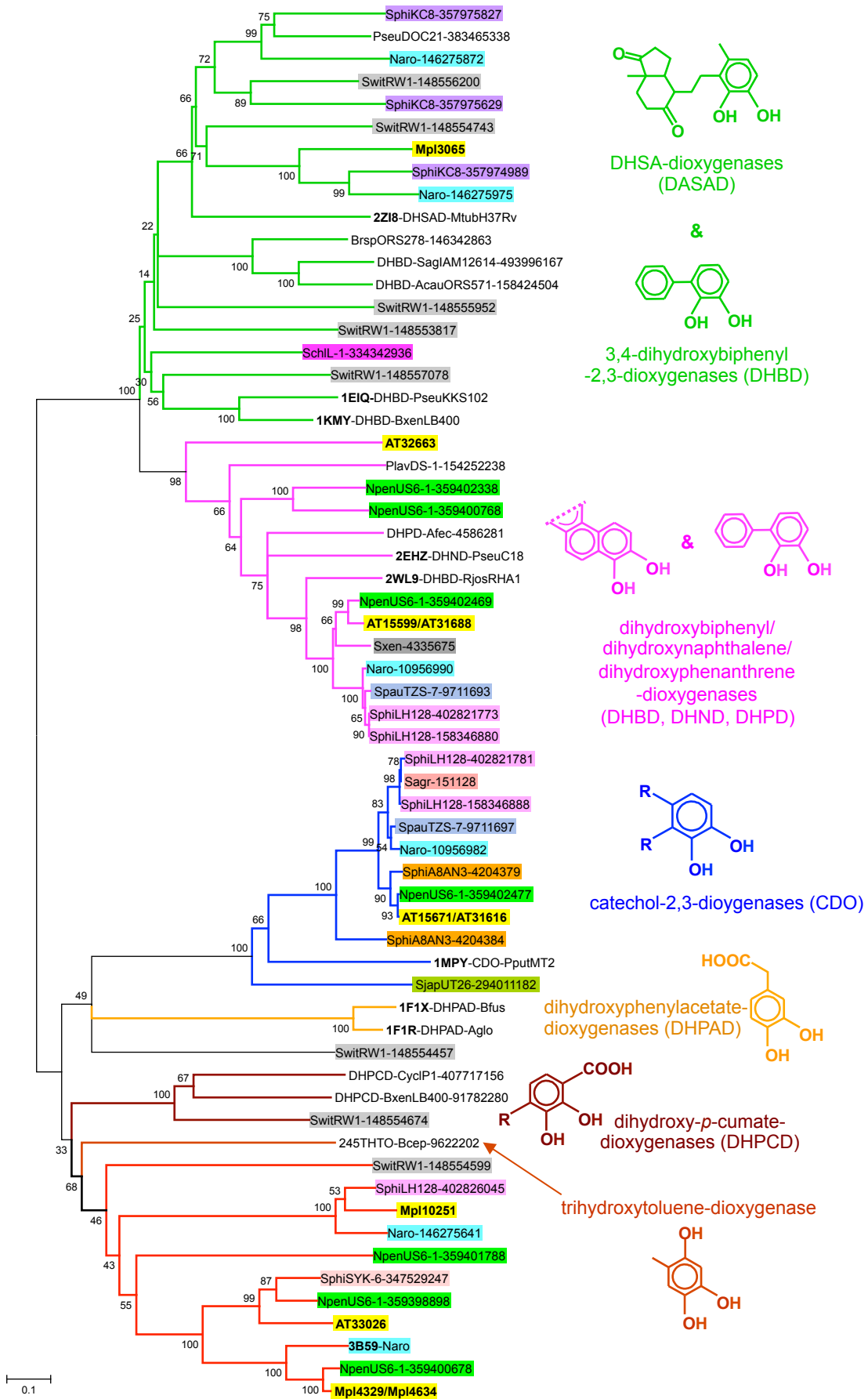


FIG S6. Neighbor-Joining tree summarizing the relationships among PP1Y RCDs (highlighted in yellow), the RCDs from several sphingomonads (each highlighted in a different color) and several other RCDs. The numbers in the names of the oxygenases refer to the *gi* accession numbers of the NCBI protein database. The PDB codes of known structures are shown in bold. Three of the PP1Y ORFs are present in double copy with a 100% identity. The AT15671/AT31616 and AT15599/AT31688 couples are located on chromosome in the pNL1 derived duplicated region B' (Supplementary Figure S3), whereas the Mpl4329/Mpl4634 couple derives from a further duplication on the megaplasmid. The analysis involved 62 amino acid sequences. All positions containing gaps were eliminated. There were a total of 189 positions in the final dataset.

Abbreviations: Naro, *N. aromaticivorans* F199; SwitRW1, *S. wittichii* RW1; NpenUS6-1, *N. pentaromativorans* US6-1; SchL1, *S. chlorophenicum* L-1; SphiKC8, *Sphingomonas* sp. KC8; SphiSYK6, *Sphingobium* sp. SYK-6; SpauTZS7 *Sphingomonas paucimobilis* TZS-7; SphiLH128, *Sphingomonas* sp. LH128; SphiA8AN3, *Sphingomonas* sp. A8AN3; Sagr, *Sphingomonas agrestis*; Sxen, *Sphingobium xenophagum*; SagIAM12614, *Stappia aggregata* IAM 12614; PseuDOC21, *Pseudomonas* sp. DOC21; CyclP1, *Cycloclasticus* sp. P1; BxenLB400, *Burkholderia xenovorans* LB400; MtubH37Rv, *Mycobacterium tuberculosis* H37Rv; PseuC18, *Pseudomonas* sp. C18; PputMT2, *Pseudomonas putida* MT2; Bfus, *Brevibacterium fuscum*; Aglo, *Arthrobacter globiformis*; RjosRHA1, *Rhodococcus jostii* RHA1; Afec, *Alcaligenes faecalis*; Bcep, *Burkholderia cepacia*; PseuKKS102, *Pseudomonas* sp. KKS102; BrspORS278, *Bradyrhizobium* sp. ORS278; AcauORS571, *Azorhizobium caulinodans* ORS 571; PlavDS-1, *Parvibaculum lavamentivorans* DS-1.

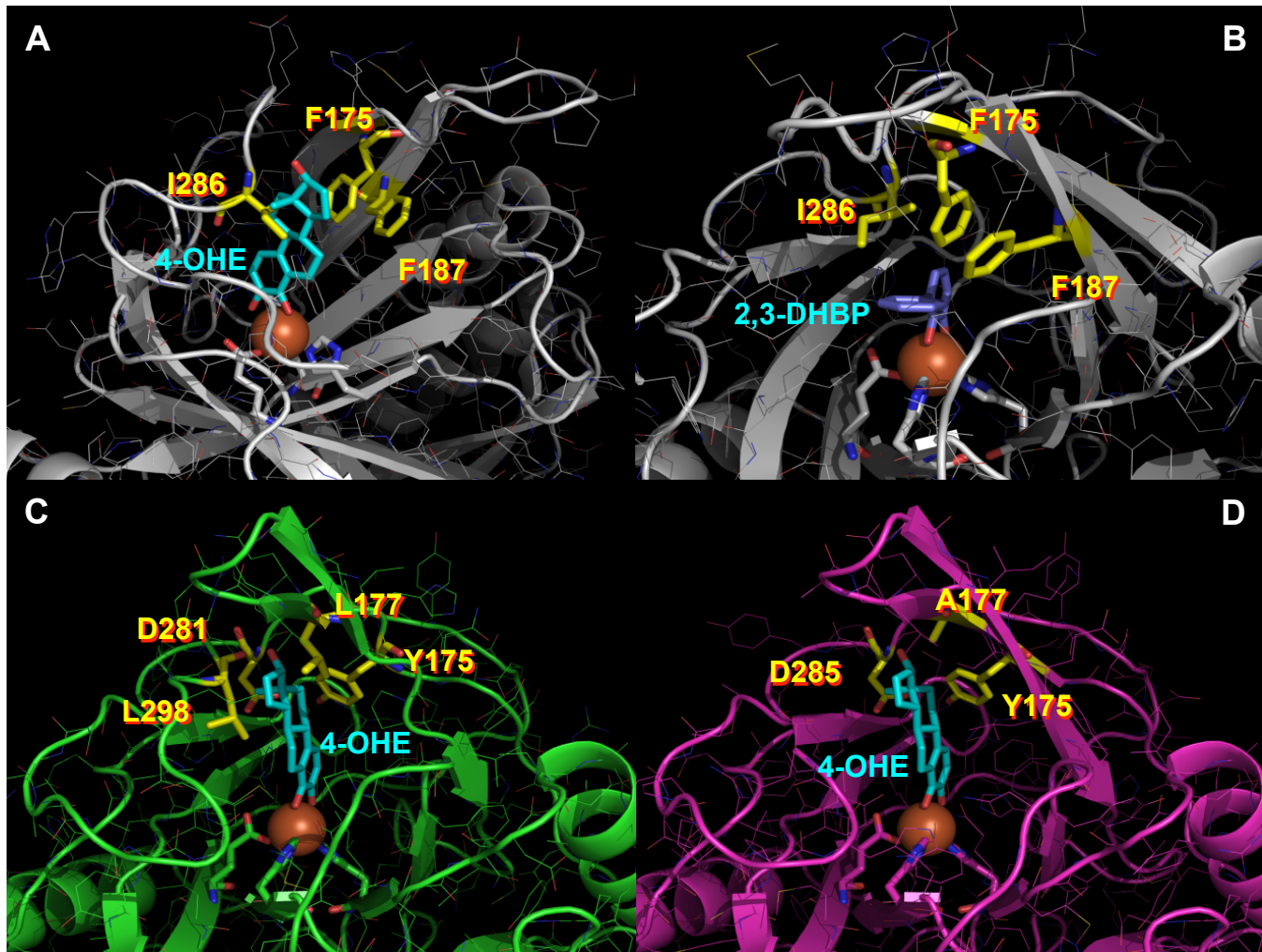


FIG S7 Homology models of PP1Y RCDs. A and B show models of the RCD coded by Mpl3065 with 4-hydroxyoestradiol (4-OHE) and 2,3-dihydroxybiphenyl (2,3-DHBP), respectively, docked into the active site. The active site of this enzyme can host only catechols with substituents at position 3 which can adopt an orientation perpendicular to the catechol ring, like 2,3-dihydroxybiphenyl, propylcatechol and isopropylcatechol. This is due to the steric hindrance of residues F175, F187 and I286 that prevent the positioning of polycyclic catechols. C and D show models of the RCDs coded by AT15599/AT31688 and AT32663, respectively, with 4-OHE docked into the active site. The active site pockets of both RCDs are wider than that of Mpl3065 and opened to the solvent. In particular, AT32663, due to a deletion of the C-terminus, has a very wide active site. Both enzymes should be able to bind substrates with 3-4 rings or larger.

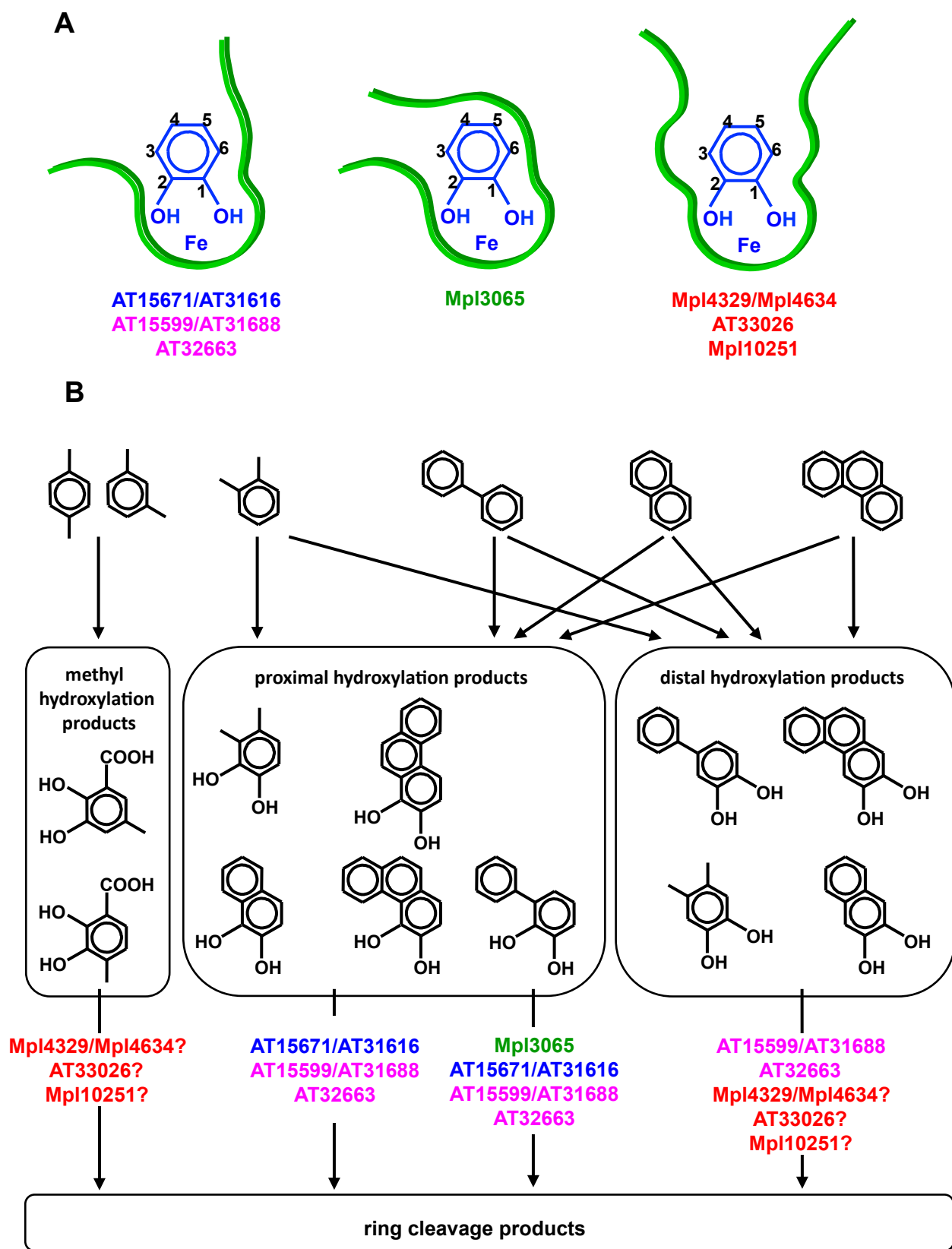
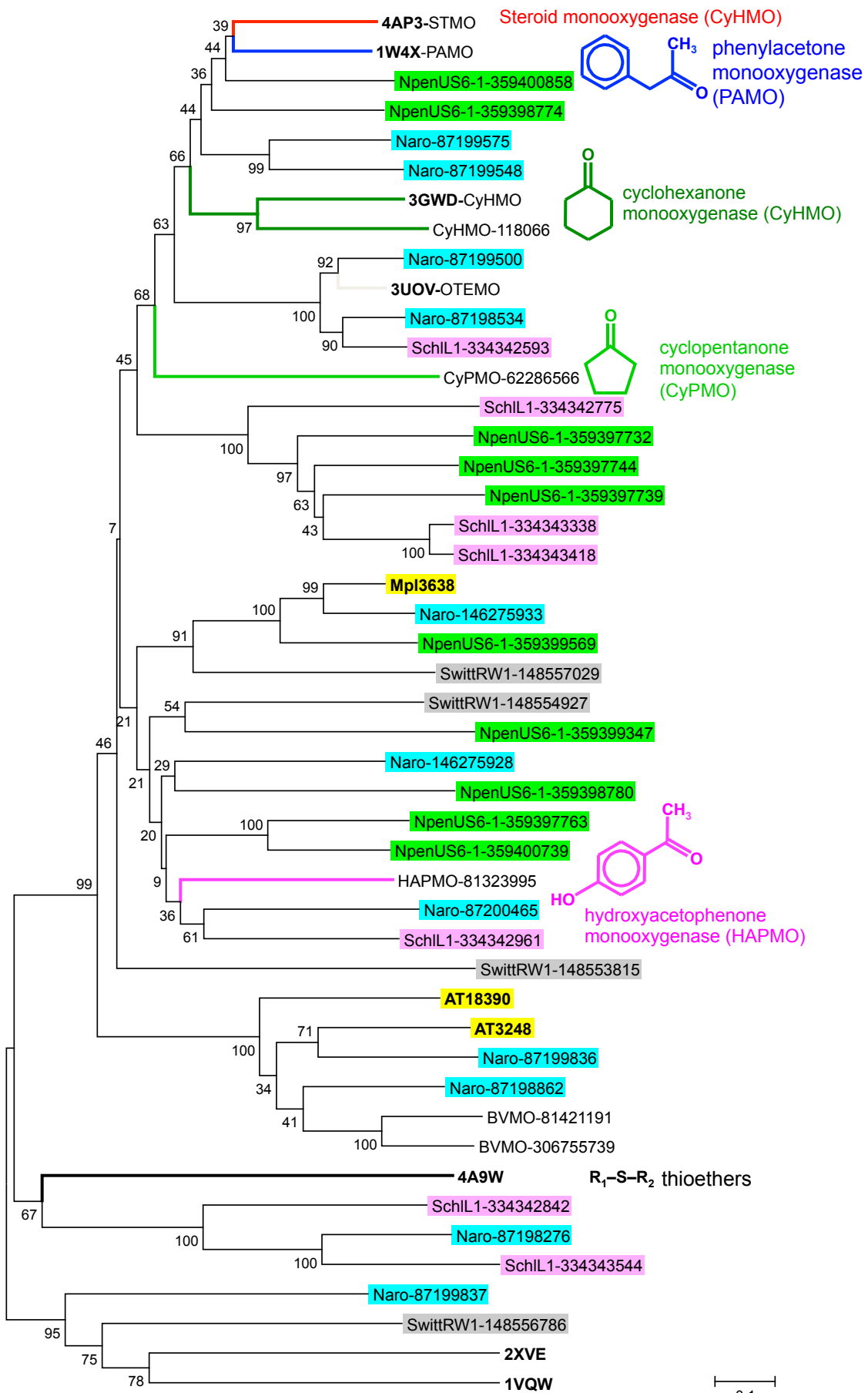


FIG S8 A) Schematic drawing of the active sites of the 7 RCDs from strain PP1Y. B) Possible metabolism of mono and polycyclic aromatic hydrocarbons during growth on complex mixtures of hydrocarbons (e.g. gasoline and diesel oil).



0,1

FIG S9 Neighbor-Joining tree summarizing the relationships among PP1Y BVMOs (highlighted in yellow), the BVMOs from several sphingomonads (each highlighted in a different color) and several other BVMOs. The numbers in the name of the oxygenases refer to the *gi* accession numbers of the NCBI protein database. PDB codes of known structures are shown in bold. The analysis involved 47 amino acid sequences. All positions containing gaps were eliminated. There were a total of 222 positions in the final dataset. OTEMO is 2-oxo- $\Delta(3)$ -4,5,5-trimethylcyclopentenyldiacetyl-CoA monooxygenase, which catalyses a key step in the metabolism of camphor by *Pseudomonas putida* ATCC 17453.

Abbreviations as in Supplementary Figure S6.

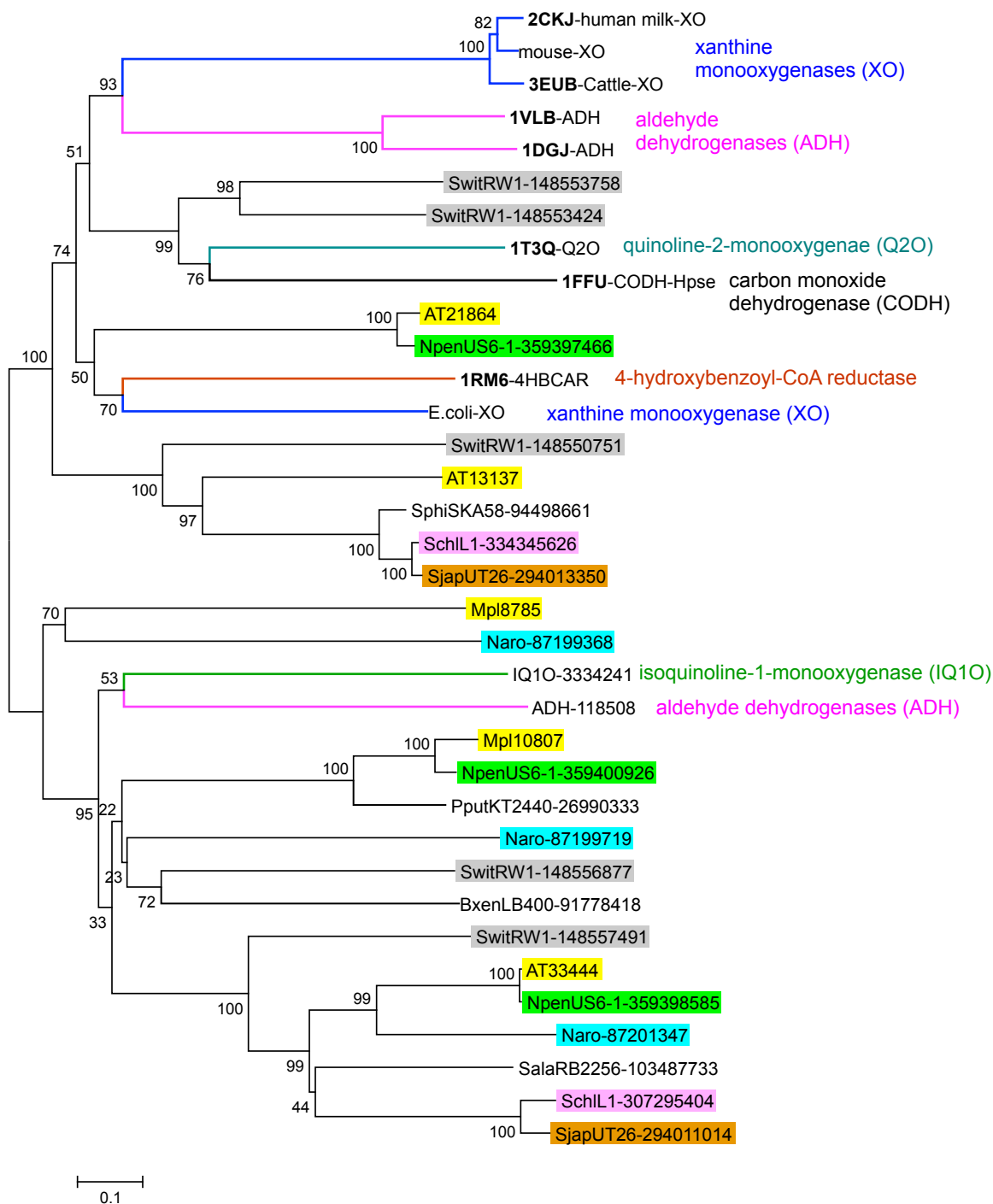


FIG S10 Neighbor-Joining tree summarizing the relationships among PP1Y MoMOs (highlighted in yellow), the MoMOs from several sphingomonads (each highlighted in a different color) and several other BVMOs. The numbers in the name of the oxygenases refer to the *gi* accession numbers of the NCBI protein database. PDB codes of known structures are shown in bold. The analysis involved 35 amino acid sequences. All positions containing gaps were eliminated. There was a total of 374 positions in the final dataset. Abbreviations: SphiSKA58, *Sphingomonas* sp; SKA58; SalaRB2256, *Sphingopyrix alaskensis* RB2256; PputKT2440, *Pseudomonas putida* KT2440. Other abbreviations are as in Supplementary Figure S6.

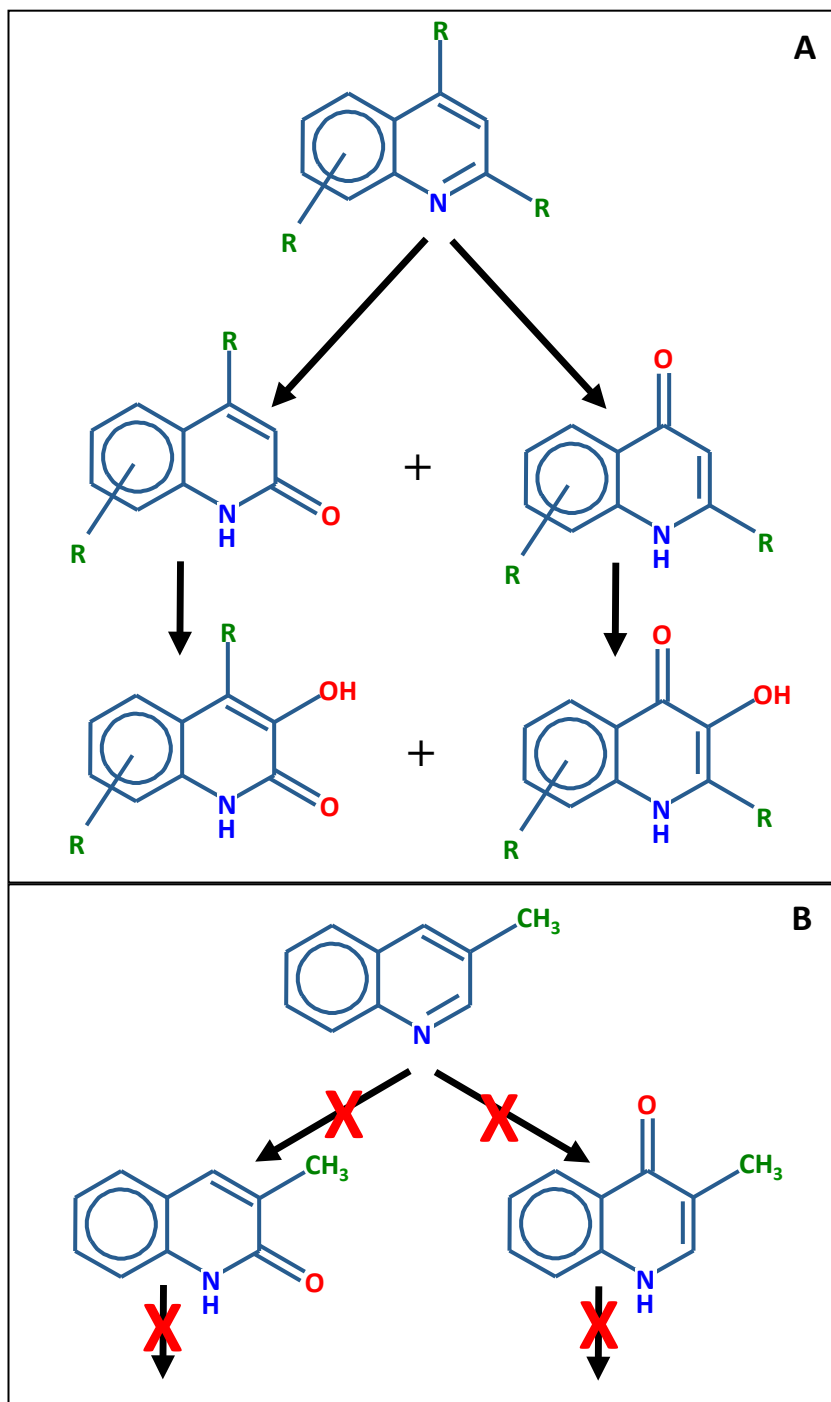


FIG S11 Hypothetical hydroxylation reactions involved in the degradation of methylquinolines. A) Initial hydroxylation at positions 2 and 4 followed by hydroxylation at position 3. Both pathways have been already described for quinoline degrading bacteria. B) A methyl group at position 3 (3-methylquinoline) could inhibit the first and or the second hydroxylation reaction, which explains why 3-methylquinoline is not a growth substrate.

B) P-type-ATPases

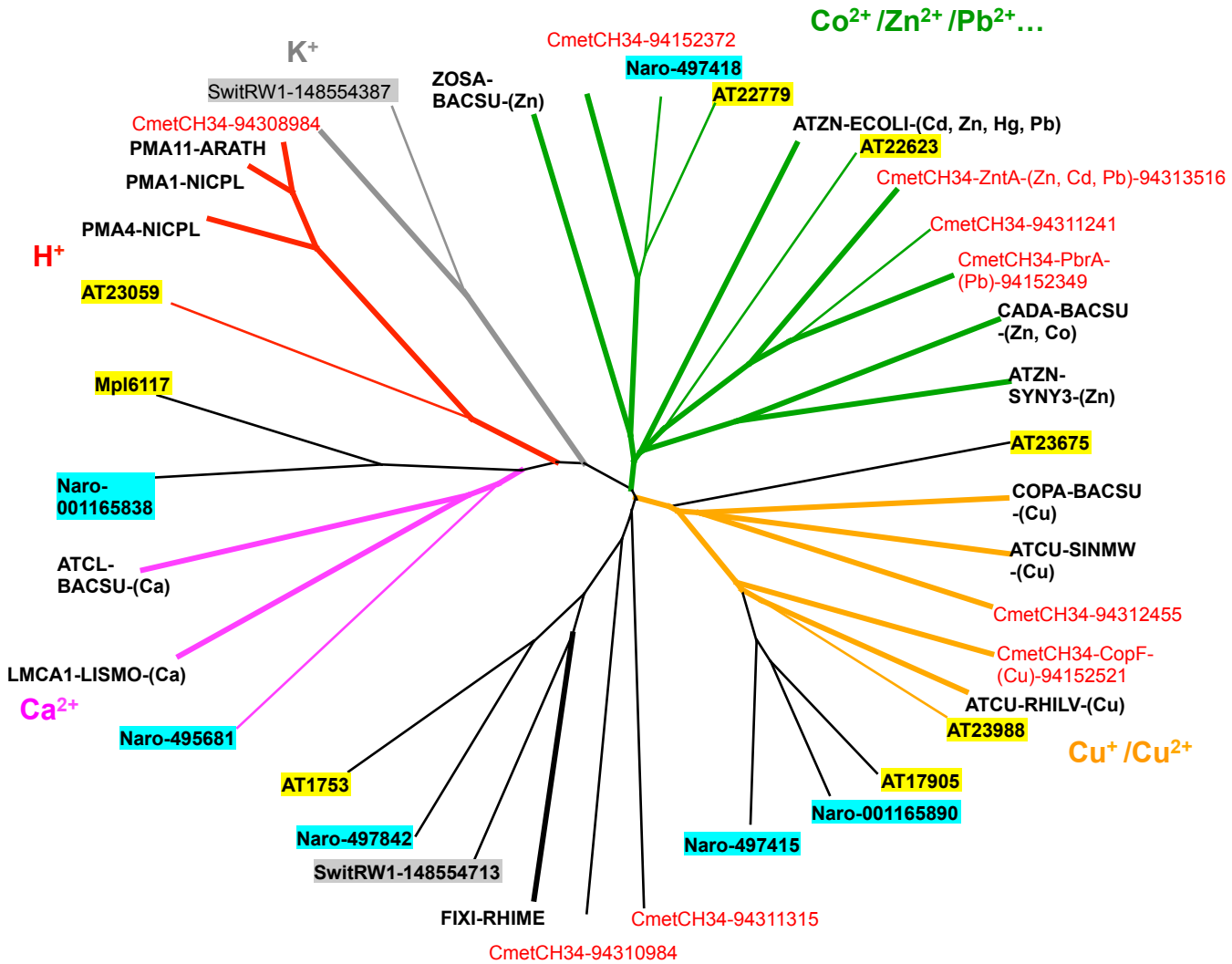


FIG S12 ClustalW tree showing the evolutionary relationships among the inner membrane subunit of RND-type efflux pumps (A) and the P-type ATPases (B). Proteins from Sphingomonads are highlighted. The numbers in the name of the oxygenases refer to the gi accession numbers of the NCBI protein database. The sequences shown in red came from *Cupriavidus metallidurans* CH34, a benchmark among the strains able to tolerate very high concentrations of transition metals.

In (A), the blue/green branch define a subfamily of RND pumps specific for neutral aromatic molecules like aromatic hydrocarbons (green branches) and acriflavine. The red/magenta branch define a subfamily of RND pumps specific for mono (magenta) and divalent (red) transition metals. None of the proteins belonging to the intermediate branches shown in black have been characterized, therefore it is not possible to speculate about the physiological role of the AT477 and AT16571 PP1Y RND-type pumps. Abbreviations: MexB-PaerPAO1, multidrug efflux transporter MexB from *Pseudomonas aeruginosa* PAO1; TTGB-PfluPf5, multidrug/solvent transporter TtgB from *Pseudomonas fluorescens* Pf-5; HAE1-PfluPf01, hydrophobe/amphiphile efflux-1 HAE1 from *P. fluorescens* Pf0-1; TTGB-Pput, toluene efflux pump TtgB from *Pseudomonas putida*; TTGB-Sodo, toluene efflux pump TtgB from *Serratia odorifera*; ACRF-EcolK12, acriflavine resistance protein F from *E. coli* K12; ACRB-EcolK12, acriflavine resistance protein B from *E. coli* K12; NCCA-Axyl, nickel-cobalt-cadmium resistance protein NccA from *Alcaligenes xylosoxydans*; CUSA-EcolK12, cation efflux system protein CusA from *E. coli* K12; BEPE-Bsui, efflux pump BepE from *Brucella suis*. *Cupriavidus metallidurans* CH34 (CmetCH34) proteins: HmuA, heavy metal cation tricomponent efflux pump; NccA, proton antiporter cation efflux protein; HmyA, heavy metal cation tricomponent efflux pump; ZneA, heavy metal cation tricomponent efflux pump; ZniA, heavy metal cation tricomponent efflux pump; CusA, copper and silver tricomponent efflux pump; SilA, proton antiporter cation efflux protein; CzcA, heavy metal efflux pump. Other abbreviation as in Supplementary Figure S6.

In (B), the orange branches define a subfamily of P-type ATPases specific for copper, the green branches a subfamily able to excrete the divalent toxic metals cobalt, nickel, lead, cadmium, mercury, and zinc, the gray branches a subfamily specific for potassium, the magenta branches a subfamily specific for calcium and the black branches uncharacterized subfamilies. The red branches define a subfamily of H⁺ transporters found only in plants. The PP1Y P-type ATPase belonging to this subfamily (coded by AT23059) was probably acquired by horizontal gene transfer. It could generate an H⁺ gradient at the expense of ATP hydrolysis thus providing energy to the H⁺ dependent RND type pumps. When known, the specificity is reported in parentheses. Abbreviations: CADA-Bsub, cadmium, zinc and cobalt-transporting ATPase from *B. subtilis*; ZOSA-Bsub, zinc transporting ATPase from *B. subtilis*; COPA-Bsub, copper-exporting ATPase A from *B. subtilis*; ATCU-Smed, copper-transporting ATPase from *Sinorhizobium medicae* WSM419; ATZN-Syne, zinc-transporting ATPase from *Synechocystis* sp. ATCC 27184; ATCU-Rleg, copper-transporting ATPase from *Rhizobium leguminosarum*; ATZN-EcolK12, lead, cadmium, zinc and mercury-transporting ATPase from *E. coli* K-12; LMCA-Lmon calcium-transporting ATPase from *Listeria monocytogenes*; ATCL-Bsub, calcium-transporting ATPase from *B. subtilis*; PMA1-Nplu, plasma membrane ATPase 1 from *Nicotiana plumbaginifolia*; PMA4-Nplu, plasma membrane ATPase 4 from *N. plumbaginifolia*; PMA11-Atha, plasma membrane-type ATPase 11 from *Arabidopsis thaliana*; FIXI-Rmel, nitrogen fixation protein FixI from *Rhizobium meliloti*. *C. metallidurans* CH34 proteins: CopF, copper efflux ATPase; PbrA, Pb(II) resistance ATPase; ZntA, ATPase involved in Zn(II), Cd(II), Tl(I) and Pb(II) resistance; CzcP, cation efflux ATPase.

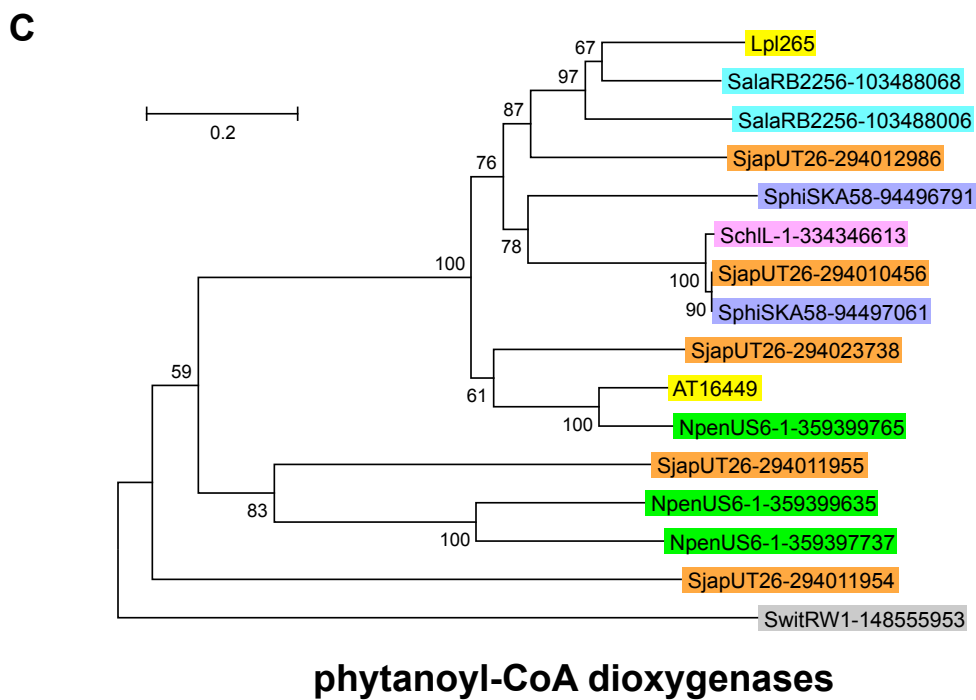
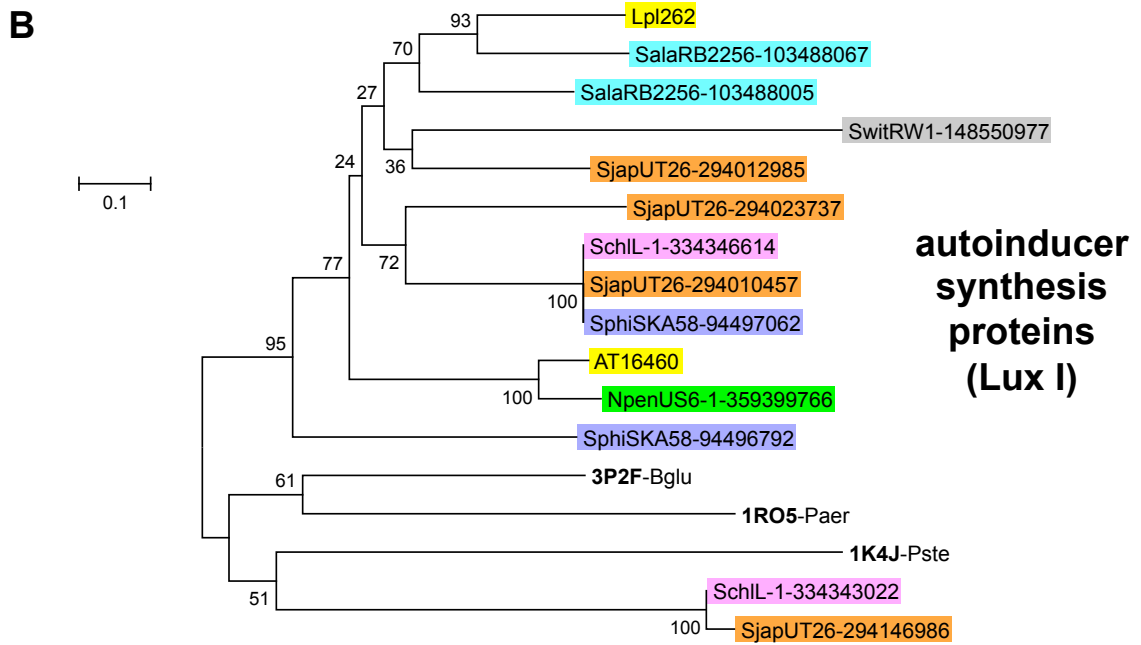
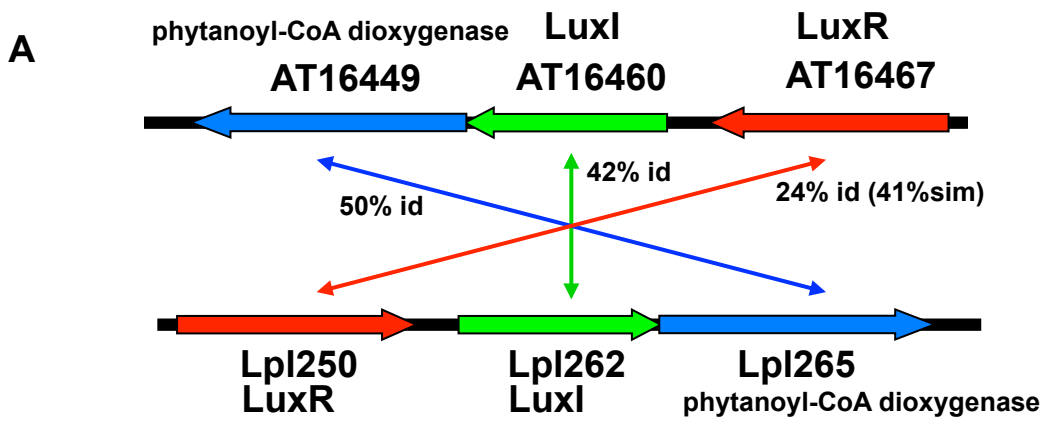


FIG S13 Cluster of the ORFs coding for LuxR, LuxI and a phytanoyl-CoA dioxygenase like protein located on chromosome and on the large plasmid Lpl (A). Neighbor-Joining tree showing the evolutionary relationships among LuxI (B) and phytanoyl-CoA dioxygenase (C) in different sphingomonads.

Abbreviation: SphiSKA58, *Sphinogomonas* sp SKA58; SalaRB2256, *Sphingopyxis alaskensis* RB2256; Bgluy,; *Burkholderia glumae*; Paer, *Pseudomonas aeruginosa*; Pste, *Pantoea stewartii*. Other abbreviations as in Supplementary Figure S6. PDB codes are shown in boldface type.

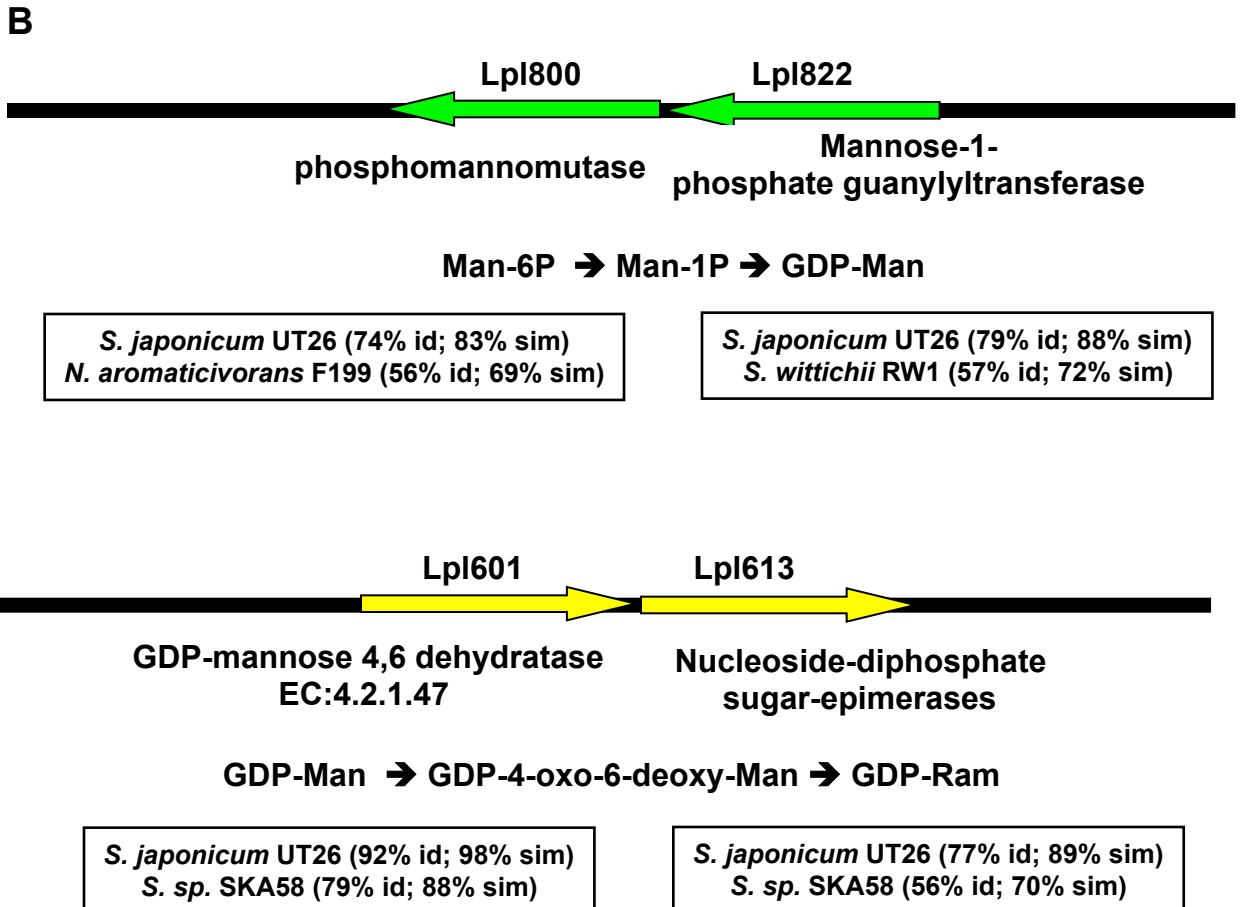
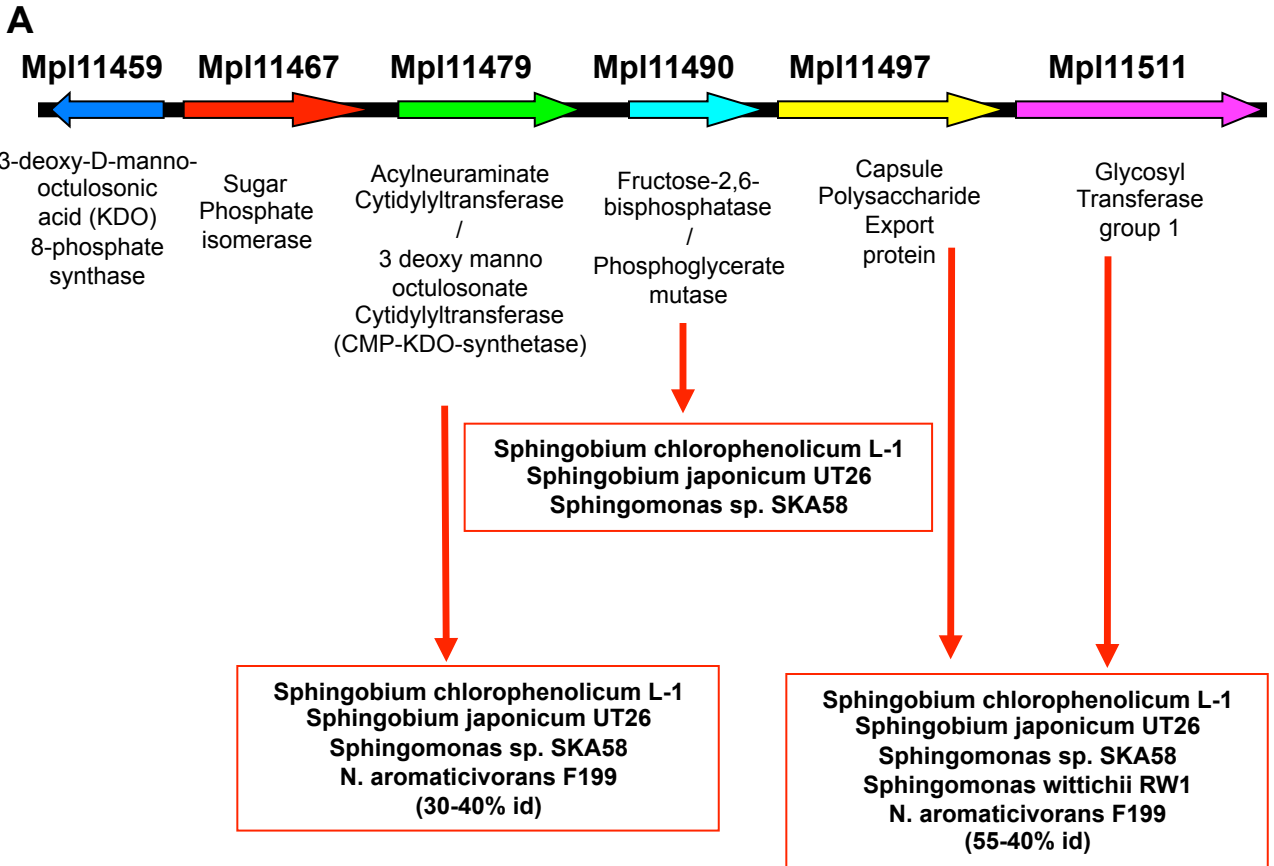
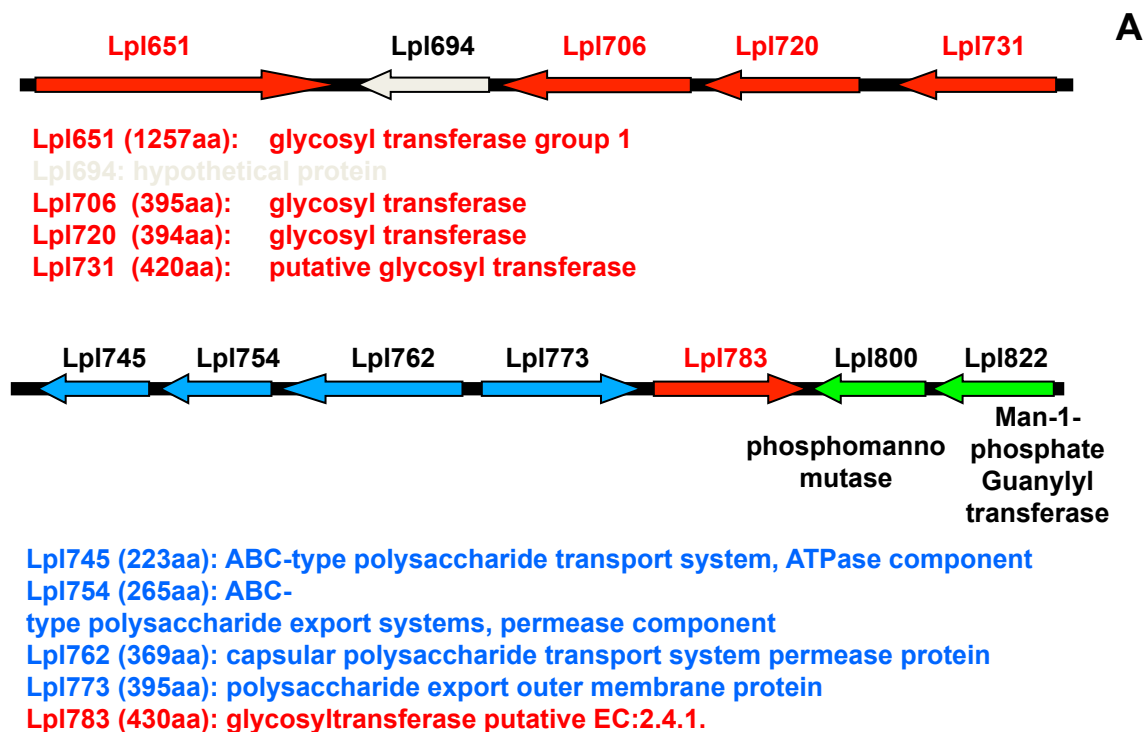


FIG S14 Clusters of ORFs potentially coding for the synthesis of extracellular polysaccharides on the Mpl (A). Regions probably involved in the synthesis of exopolysaccharides on the Lpl (B). Two close couples of ORFs code for the enzymes necessary for the synthesis of the precursors GDP-mannose and GDP-rhamnose, i.e., the products of Lpl800 and Lpl822 convert mannose-6-phosphate to GDP-mannose, whereas the products of Lpl601 and Lpl613 convert GDP-mannose to GDP-rhamnose.



B

Lpl651: Not present in other sphingomonadas

Lpl706: Only in *S. japonicum* UT26 (29% id)

Lpl720: Not present in other sphingomonadas

Lpl731: Not present in other sphingomonadas

Lpl745: *N. aromaticivorans* F199 (69% id; 86% sim); *S. sp.* SKA58 (55% id; 73% sim)

Lpl754: *S. japonicum* UT26 (83% id; 92% sim); *N. aromaticivorans* F199 (65% id; 82% sim); *S. sp.* SKA58 (56% id; 77% sim); *S. wittichii* RW1 (36% id; 56% sim)

Lpl762: *S. japonicum* UT26 (73% id; 86% sim); *S. sp.* SKA58 (59% id; 76% sim); *N. aromaticivorans* F199 (51% id; 70% sim); *S. wittichii* RW1 (34% id; 52% sim)

Lpl773: *S. japonicum* UT26 (68% id; 80% sim); *N. aromaticivorans* F199 (51% id; 70% sim); *S. sp.* SKA58 (50% id; 66% sim)

Lpl783: Only in *S. japonicum* UT26 (65% id; 76% sim)

FIG S15 Lpl ORFs coding for glycosyl transferases and 4 subunits of an ABC-type polysaccharide transport system (A) and their homology with other sphingomonads (B). A close homologue of the hypothetical glycosyl transferase Lpl783 was found in *S. japonicum* UT26, whereas only very distantly related homologues of glycosyl transferases Lpl706, Lpl720 and Lpl731 can be found among sphingomonads.

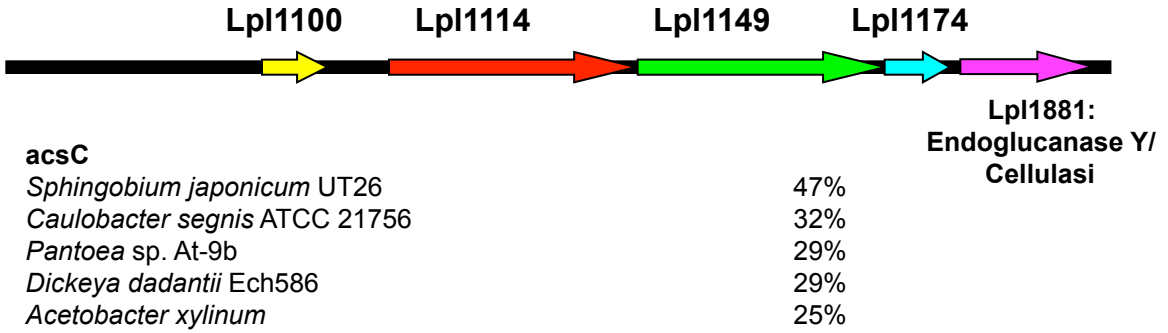
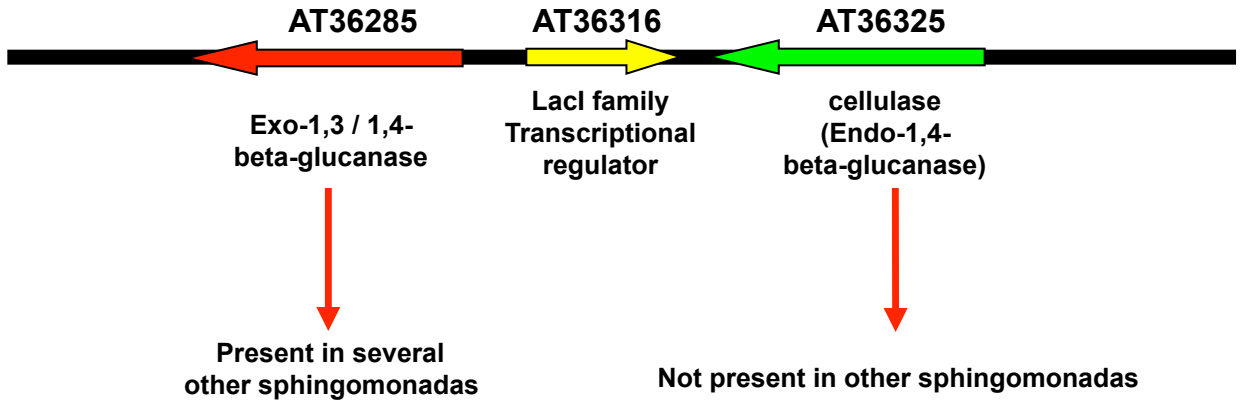
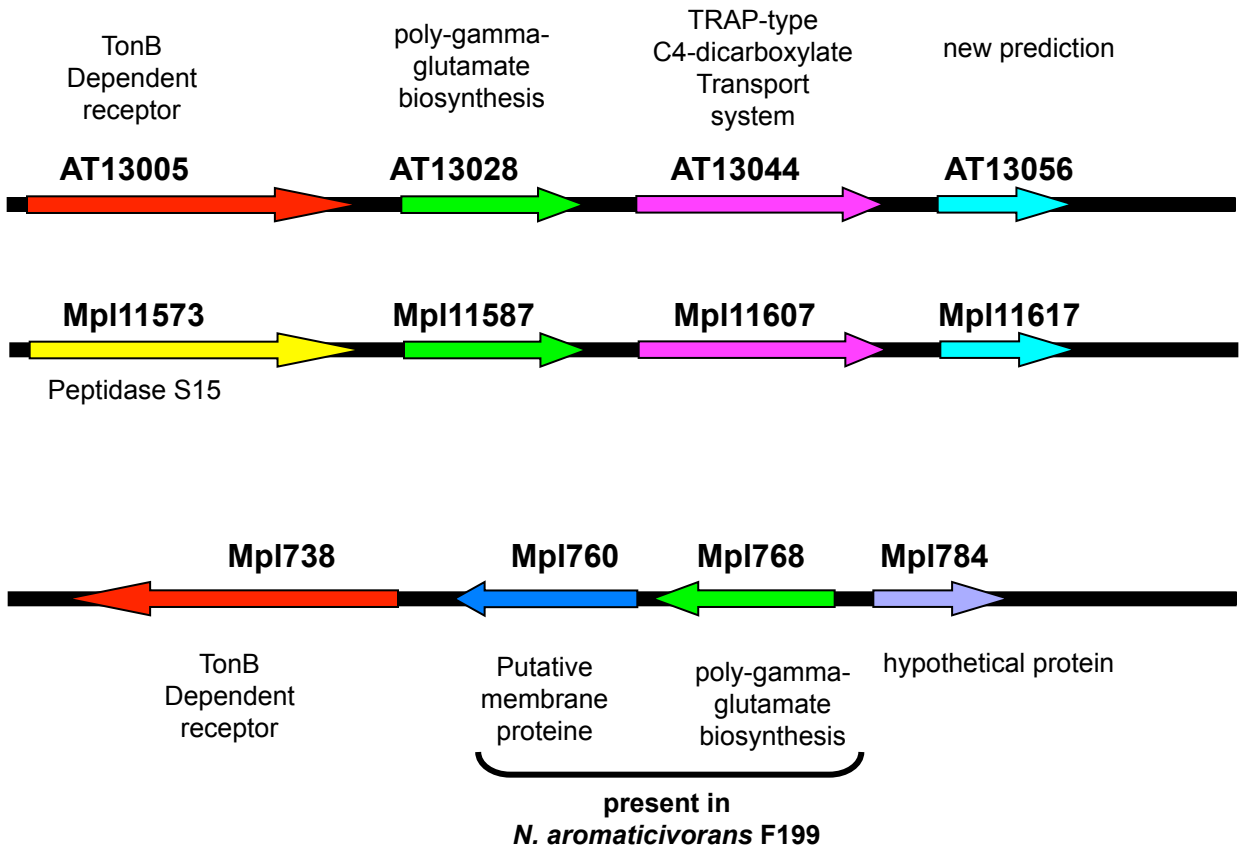
A**B****C**

FIG S16 Lpl ORFs coding for a cellulose synthase and a hypothetical cellulose (A). Chromosome ORF coding for a hypothetical cellulase (AT36325) near to an ORF coding for an exo-1,3/1,4-beta-glucanase (B). ORFs coding for γ -PGA polymerases (C). One of these ORFs (Mpl768) is adjacent to an ORF coding for a hypothetical membrane protein. The same couple of ORFs is present in the genome of *N. aromaticivorans* F199 but not in other sphingomonads. The other two ORFs are part of two similar clusters of three ORFs located on the chromosome and megaplasmid. Interestingly, this cluster is not present in other sphingomonads.